

MODELLING OF FIXED BED CATALYTIC REACTORS CATALYST POISONING

Jozef MARKOŠ, Alena BRUNOVSKÁ and Ján ILAVSKÝ

*Department of Organic Technology,
Slovak Institute of Technology, 812 37 Bratislava*

Received January 14th, 1985

The paper deals with modelling of catalytic reactors in which an irreversible catalyst deactivation takes place. The dimensionless model equations are derived for heterogeneous models of well-mixed regions in series, an algorithm for their solution is proposed. The obtained results are compared with experimental ones in the case of hydrogenation of benzene on a nickel catalyst with thiophene as a poison.

Catalyst deactivation is one of the principal problems in catalyst development and design of fixed bed catalytic reactors. It leads to a decrease of the performance of the reactor which requires regeneration or replacement of the catalyst in certain intervals. That means a stand-still of the reactor and results in production loss and increase of running cost.

In our previous papers¹⁻³ pseudohomogeneous models of fixed bed catalytic reactor in which an irreversible chemisorption of catalyst poison (from some impurity in the feed) takes place have been discussed. The chemisorption rate of the poison has been considered equal on all nonoccupied active sites and expressed by a Langmuir-type rate equation. As a flow pattern the plug flow¹, well-mixed regions in series² and axial dispersion model³ have been chosen.

In this paper heterogeneous models of well-mixed regions in series are studied. As a poisoning mechanism three cases are considered: 1) uniform mechanism with one type of active sites; 2) uniform mechanism with two types of active sites; 3) shell progressive mechanism. Theoretical results are compared with experimental ones for the model system (hydrogenation of benzene on a nickel catalyst with thiophene as the poison).

THEORETICAL

Heterogeneous Model of Well-Mixed Regions in Series

The models of fixed bed catalytic reactor developed below are valid under the following assumptions: a) Intrepellet gradients can be neglected, the concentrations

and temperature inside the pellets are equal to the surface ones. *b*) The deactivation rate is much lower than the rate of the catalytic reaction, *i.e.* quasi-steady state assumption is considered. *c*) The catalyst poison concentration is considerably lower than the concentration of the key component, so the heat released by the chemisorption of the poison compared to the heat released by the catalytic reaction is negligible. *d*) The gas density is constant. *e*) The heat of the reaction, heat capacity, mass transfer and heat transfer coefficients are temperature independent. *f*) The deactivation process is temperature independent. *g*) The catalyst pellets are spherical. *h*) The rate equation is separable⁴. *i*) Catalyst activity depends linearly on the adsorbed amount of the poison.

The model consists of:

material balance equations for the key component

$$\dot{V}_{i-1}c_{B_{i-1}}^* - k_{gB}a_{vi}(c_{B_i}^* - c_{B_i}^p) = \dot{V}_i x_{B_i}^* \quad (\text{fluid}) \quad (1)$$

$$k_{gB} 4\pi R^2(c_{B_i}^* - c_{B_i}^p) = -\frac{4}{3}\pi R^3 \rho_s v_B \dot{\xi}_w \quad i = 1, \dots, N \quad (\text{solid}) \quad (2)$$

material balance equations for the poison

$$\dot{V}_{i-1}c_{J_{i-1}}^* - k_{gJ}a_{vi}(c_{J_i}^* - c_{J_i}^p) = \dot{V}_i c_{J_i}^* \quad (\text{fluid}) \quad (3)$$

$$k_{gJ} 4\pi R^2(c_{J_i}^* - c_{J_i}^p) = \frac{4}{3}\pi R^3 \rho_s \frac{da_J}{dt} \quad (\text{solid}) \quad i = 1, \dots, N \quad (4)$$

enthalpy balances

$$\dot{V}_{i-1}\rho_g c_{pg} T_{i-1}^* + h_w A_{wi}(T_c - T_i^*) - h_f a_{vi}(T_i^* - T_i^p) = \dot{V}_i \rho_g c_{pg} T_i^* \quad (\text{fluid}) \quad (5)$$

$$h_f 4\pi R^2(T_i^* - T_i^p) = -\frac{4}{3}\pi R^3 \rho_s (-\Delta H) \dot{\xi}_w \quad (\text{solid}) \quad i = 1, \dots, N \quad (6)$$

rate equation of the catalytic reaction

$$\dot{\xi}_w = \Phi f(c_A, c_B, \dots, T) \quad (7)$$

rate equation of the poison chemisorption

$$\dot{a} = \dot{a}(\Phi, c_J, T) \quad (8)$$

boundary conditions

$$i = 1, \quad t > 0, \quad c_{B_{i-1}}^* = c_{B_0}, \quad c_{J_{i-1}}^* = c_{J_0}, \quad T_{i-1}^* = T_0^* \quad (9)$$

The initial conditions are given by the solution of Eqs (1)–(9) for the fresh catalyst.

The chemisorption rate equation depends on the assumption on the deactivation mechanism. Two limit cases are to be considered⁵: the so-called “uniform” and “shell progressive” decay mechanism.

In the uniform mechanism the resistance to diffusion of poison is negligible and poison deposits uniformly and progressively throughout the pellet. This can be expected for small catalyst pellets with large pore diameter and for low rates of the poison chemisorption. On the other hand, if the resistance to pore diffusion hinders the flow of poison into the pellet then the poison deposits preferentially near the exterior surface of the pellet. If the resistance to diffusion or the affinity of the poison to the catalytic surface is high, the poison deposits in a thin and growing shell at the surface of the pellet. This mechanism can be expected for large pellets with long narrow pores and at high rate of the poison chemisorption.

In this study two types of uniform mechanisms are treated: homogeneous mechanism with a unique type of active sites and a two site model.

Model 1: Shell Progressive Mechanism of Deactivation

In this model we assume that the pellet consists of an unpoisoned core with unit activity surrounded by a poisoned shell with zero activity. For the mathematical description of the deactivation process in the catalytic reactor it is necessary to know the speed of movement of the border between the active core and nonactive shell. For the decrease of the active core radius the following relation has been developed⁶:

$$\frac{dr^j}{dt} = - \frac{k_s}{a_j^* \rho_s} \frac{c_j^*}{1 + k_s r^{j2} / (k_g R^2) + r^j (R - r^j) / (D_j R)} \quad (10)$$

After introducing dimensionless variables it becomes

$$\frac{d\varphi}{d\tau} = - \frac{Y_j^*}{\omega_{11} + \omega_{12} \varphi^2 + \omega_{13} \varphi (1 - \varphi)} \quad (11)$$

and the rate of deactivation is

$$\frac{d\Phi}{dt} = - \frac{1}{a_j^*} \frac{da_j}{dt} = 3\varphi^2 \frac{d\varphi}{dt} \quad (12)$$

The model includes chemisorption, external diffusion and diffusion through the shell of ratio $\omega_{11} : \omega_{12} : \omega_{13}$.

The system of model equations in the dimensionless form of the heterogeneous model of well-mixed regions in series using shell progressive mechanism of deactivation is:

material balances of the key component

$$Y_{Bi-1}^* - Z_{gi}(Y_{Bi}^* - Y_{Bi}^p) = Y_{Bi}^* \quad i = 1, \dots, N \quad (13)$$

$$Y_{Bi}^* - Y_{Bi}^p = Z_s \dot{\xi} \quad (14)$$

material balances of the poison

$$Y_{Ji-1}^* - G_{gi}(Y_{Ji}^* - Y_{Ji}^p) = Y_{Ji}^* \quad (15)$$

TABLE I

Experimental conditions

Run	1	2	3	4	5
Catalyst diameter [10^3 m]	1.25—1.4	1.25—1.4	1.0—1.25	1.0—1.25	0.7—1.0
Catalyst mass [g]	15.03	14.08	13.05	12.1	11.64
Inlet temperature [$^{\circ}$ C]	71	91.7	73.1	103.6	105
Ambient temperature [$^{\circ}$ C]	71	91.7	73.1	103.6	105
Volumetric flow rate [10^6 m ³ s ⁻¹]	2.207	2.208	3.929	3.937	5.445
Inlet benzene concentration [mol m ⁻³]	2.04	1.958	2.063	1.892	1.898
Inlet thiophene concentration [mol m ⁻³]	6.683	3.591	3.721	3.812	2.699
Length of bed [m]	0.12	0.105	0.102	0.121	0.085

TABLE II

Parameters of the rate equation

$$\begin{aligned}
 k_{\infty} &= 5.882 \cdot 10^{-3} \text{ mol kg}^{-1} \text{ s}^{-1} \text{ Pa}^{-1} \\
 K_{\infty} &= 2.866 \cdot 10^{-6} \text{ Pa}^{-1} \\
 E &= 3.536 \cdot 10^4 \text{ J mol}^{-1} \\
 Q &= -2.422 \cdot 10^4 \text{ J mol}^{-1} \\
 (-\Delta H) &= 2.09 \cdot 10^5 \text{ J mol}
 \end{aligned}$$

$$Y_{ji}^* - Y_{ji}^p = -3G_{s1}\varphi^2 \frac{d\varphi}{d\tau} \quad i = 1, \dots, N \quad (16)$$

enthalpy balances

$$\Theta_{i-1}^* + F_{wi}(\Theta_c - \Theta_i^*) - F_{ri}(\Theta_i^* - \Theta_i^p) = \Theta_i^* \quad i = 1, \dots, N \quad (17)$$

$$\Theta_i^* - \Theta_i^p = -F_s \dot{\xi} \quad (18)$$

rate equation of the catalytic reaction

$$\dot{\xi} = \Phi f(Y_A, Y_B, \dots, \Theta) \quad (19)$$

deactivation rate Eq. (11)

boundary and initial conditions

$$i = 1, \quad \tau > 0, \quad Y_{Bi-1}^* = Y_{ji-1}^* = 1, \quad \Theta_{i-1}^* = 0. \quad (20)$$

Model 2: Uniform Mechanism of Deactivation with One Type of Active Sites

The deactivation is caused by irreversible poison adsorption on the active sites resulting in their gradual occupancy for the catalytic reaction. Assuming that the adsorption rate of the poison is equal for all active sites (regardless of whether

TABLE III
Values of model parameters

Run	1	2	3	4	5
k_{gB} [m s^{-1}]	0.01365	0.01453	0.02000	0.02180	0.02970
k_{gJ} [m s^{-1}]	0.01031	0.01089	0.01509	0.0163	0.02216
h_f [$\text{J m}^{-2} \text{K}^{-1} \text{s}^{-1}$]	143.5	137.7	209.3	198.8	268.4
k_D [$\text{mol m}^{-3} \text{s}^{-1}$]	0.08083	0.1034	0.0830	0.1176	0.1194
k_{D1} [$\text{mol m}^{-3} \text{s}^{-1}$]	0.09565	0.1197	0.0975	0.1263	0.1276
γ	0.2228	0.2228	0.2229	0.2228	0.2228
f	0.5367	0.5367	0.5367	0.5367	0.5367
k_s [m s^{-1}]	0.05561	0.0793	0.0578	0.0956	0.0976
D_J [$\text{m}^2 \text{s}^{-1} \cdot 10^3$]	0.308	0.4828	0.323	0.6116	0.628
h_W [$\text{J m}^{-2} \text{K}^{-1} \text{s}^{-1}$]	244	424	181.1	522	378
N	90	79	90	80	98
a_j^* [mol kg^{-1}]	0.3619	0.3463	0.3517	0.4514	0.4809

they are free or whether reactants or products are adsorbed on them) and just one molecule of poison is adsorbed on one active site by Langmuir rate equation one can write

$$\frac{d\Phi}{dt} = \frac{k_D \Phi c_J^*}{1 + k_D R Q_s a_J^* \Phi / (3k_{gJ})} \quad (21)$$

Transforming Eq. (21) to dimensionless form it becomes

$$\dot{\Phi} = d\Phi/d\tau = - \frac{Y_J^* \Phi}{\omega_{21} + \omega_{22} \Phi} \quad (22)$$

In this case only external diffusion and chemisorption are considered, their ratio being $\omega_{21} : \omega_{22}$.

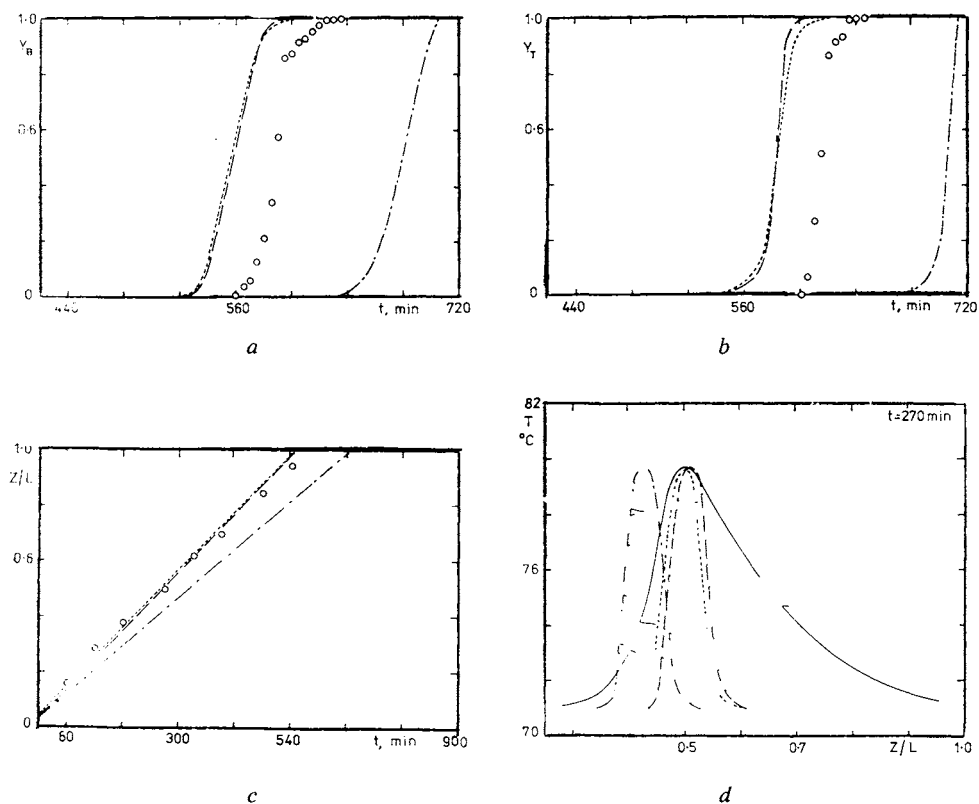


FIG. 1

Comparison of experimental and computed dependences. Run 1. \circ Experiment, ----- Model 2, - · - · - Model 1, ······ Model 3, a) Exit benzene concentration vs time. b) Exit thiophene concentration vs time. c) Point of temperature peak vs time. d) Transient temperature profiles

The system of model equations in the dimensionless form of the heterogeneous model of well-mixed region in series with uniform deactivation mechanism of catalyst is described by material balances of the key component (13), (14), enthalpy balances (17), (18) and the balances of the poison

$$Y_{j_{i-1}}^* - G_{gi}(Y_{j_i}^* - Y_{j_i}^p) = Y_{j_i}^*, \quad i = 1, \dots, N. \quad (23)$$

$$Y_{j_i}^* - Y_{j_i}^p = G_{s2}\phi \quad (24)$$

The deactivation rate equation is given by Eq. (22), the reaction rate by Eq. (19) and the boundary and initial conditions

$$i = 1, \quad \tau > 0, \quad Y_{B_{i-1}}^* = Y_{j_{i-1}}^* = 1, \quad \Theta_{i-1}^* = 0 \quad (25)$$

$$\tau = 0, \quad \phi_i = 1, \quad i = 1, \dots, N.$$

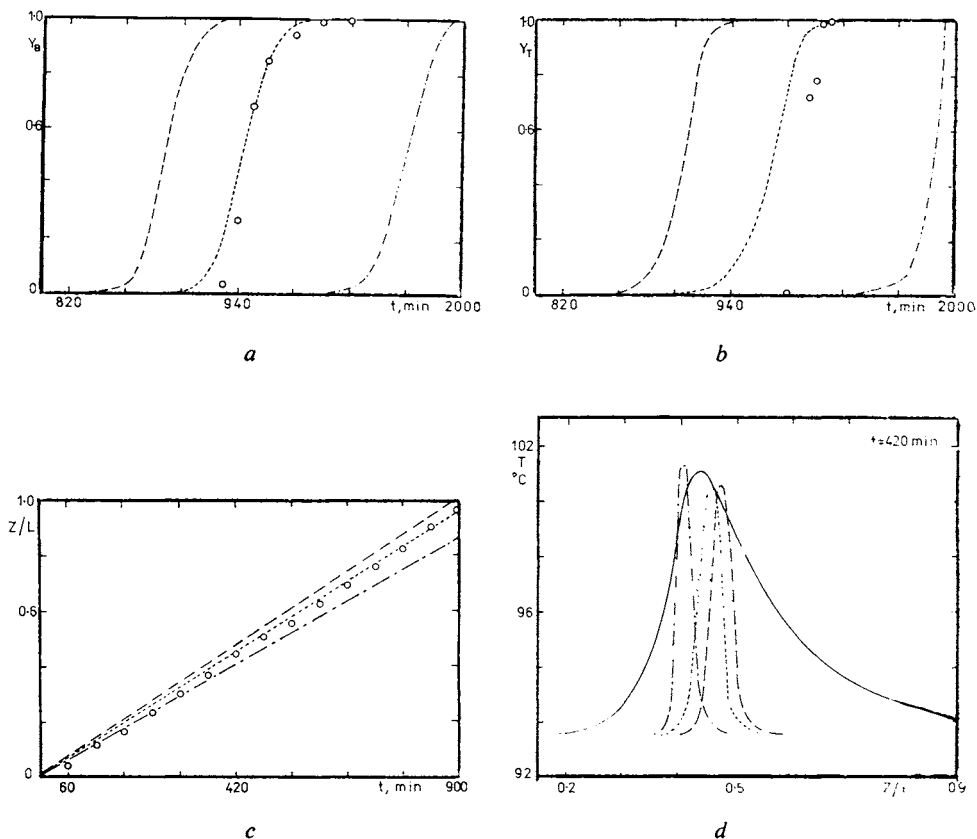


FIG. 2

Comparison of experimental and computed dependences. Run 2. Notation as in Fig. 1

Model 3: Uniform Mechanism of Deactivation with Two Types of Active Sites

In this mechanism two types of active sites on the catalyst surface are to be considered: *a*) active sites for catalytic reaction and for poison chemisorption; *b*) active sites for chemisorption alone (*i.e.* inactive in catalytic reaction).

The activity decrease rate and the rate of the poison chemisorption are given by

$$\frac{d\Phi}{dt} = - \frac{k_{D1}c_J^*\Phi}{1 + (\rho_s R a_J^* k_{D1}) (\gamma\Phi + f(1-\gamma)\Phi^f) / Jk_{gJ}} \quad (26)$$

and

$$\frac{da_J}{dt} = \frac{a_J^* k_{D1} c_J^* [\gamma\Phi + f(1-\gamma)\Phi^f]}{1 + (\rho_s R a_J^* k_{D1}) (\gamma\Phi + f(1-\gamma)\Phi^f) / 3k_{gJ}} \quad (27)$$

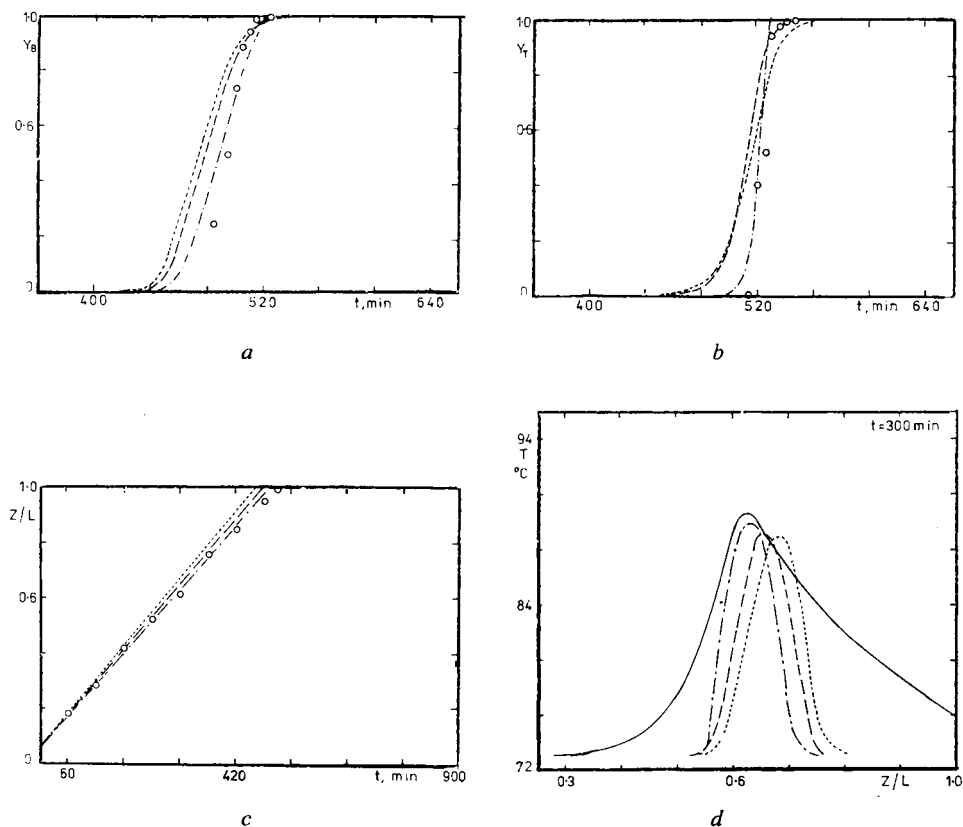


FIG. 3

Comparison of experimental and computed dependences. Run 3. Notation as in Fig. 1

After introducing dimensionless variables Eqs (26) and (27) becomes

$$\dot{\Phi} = - \frac{Y_J^*}{\omega_{31} + \omega_{32}(\gamma\Phi + f(1-\gamma)\Phi^f)} \quad (28)$$

and

$$\frac{dA_J}{d\tau} = \frac{Y_J^*(\gamma\Phi + f(1-\gamma)\Phi^f)}{\omega_{31} + \omega_{32}(\gamma\Phi + f(1-\gamma)\Phi^f)}. \quad (29)$$

The parameters ω_{31} and ω_{32} correspond to the parameters ω_{21} and ω_{22} in model 2.

The system of the model equations of the model of well-mixed regions in series and two site model for poison chemisorption consists of the balances (13), (14), (17).

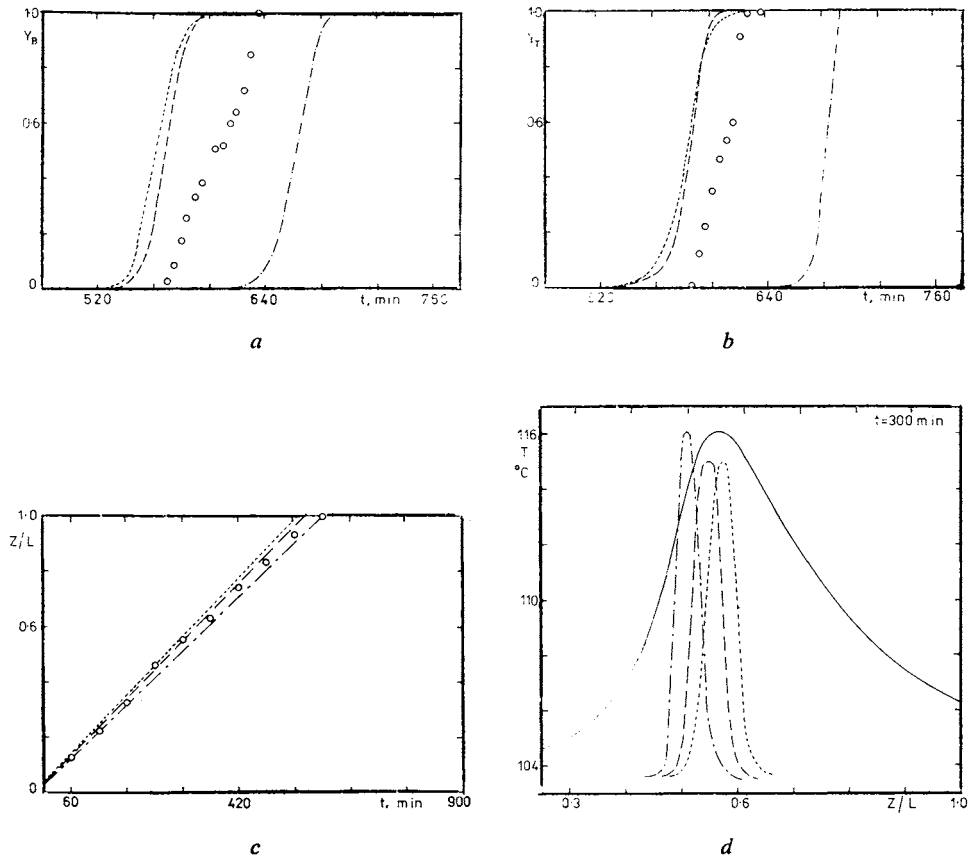
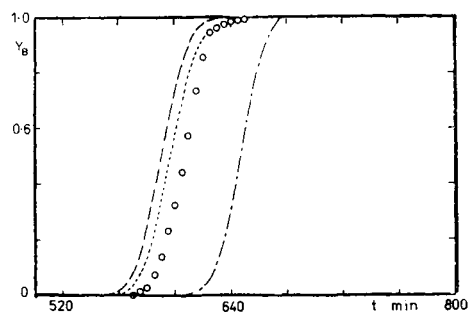


FIG. 4

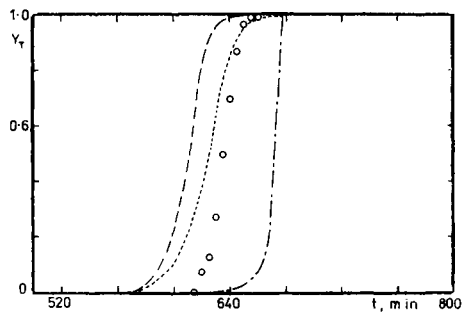
Comparison of experimental and computed dependences. Run 4. Notation as in Fig. 1

TABLE IV
Time instances in which exit benzene concentration is equal to 0.5

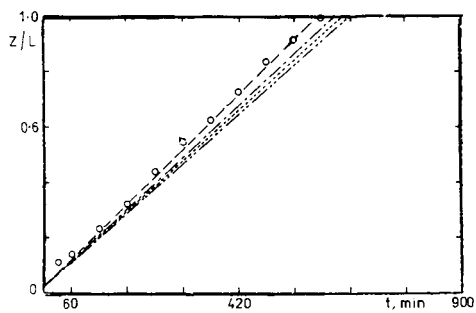
Run	$t^{1/2}$ exp min	$t^{1/2}$, Model 1 min	δ %	$t^{1/2}$, Model 2 min	δ %	$t^{1/2}$, Model 3 min	δ %
1	588.3	679.2	15.5	558.6	5	556.4	5.4
2	945.4	1 059.0	10.7	887.5	6.1	9.41.7	0.4
3	495.1	488.1	2	479.0	3.2	473.2	4.4
4	604.1	661.6	9.5	568.8	5.9	561.5	7.1
5	607.1	647.5	11.1	591.0	2.7	595.0	2.0
		$\bar{\delta}$ 9.8		$\bar{\delta}$ 4.6		$\bar{\delta}$ 3.9	



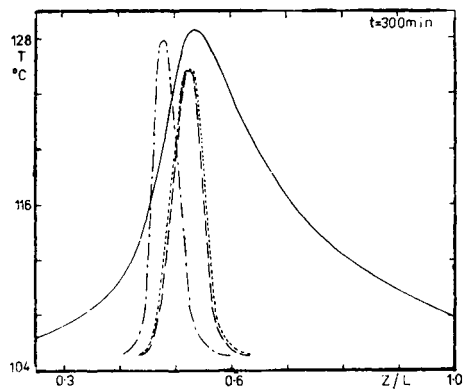
a



b



c



d

FIG. 5
Comparison of experimental and computed dependences. Run 5. Notation as in Fig. 1

(18), the balances of the poison

$$Y_{ji}^* - G_{gi}(Y_{ji}^* - Y_{ji}^p) = Y_{ji}^* \quad (30)$$

$$Y_{ji}^* - Y_{ji}^p = + G_{s3} \frac{Y_{ij}^*(\gamma\Phi_i + f(1-\gamma)\Phi_i^f)}{\omega_{31} + \omega_{32}(\gamma\Phi_i + f(1-\gamma)\Phi_i^f)} \quad (31)$$

$$i = 1, \dots, N$$

the rate equations (19), (29) and boundary and initial conditions (25).

Rate Equation

The rate equation of the catalytic reaction is⁷

$$\dot{\xi}_w = \Phi \frac{k_\infty K_\infty P_B P_H \exp[-(Q+E)/(RT)]}{1 + K_\infty P_B \exp - Q/(RT)} \quad (32)$$

or, in the dimensionless form

$$\dot{\xi} = \Phi \frac{(1 + \kappa_B) Y_B Y_H \exp[(\alpha_i + \alpha_k) \beta \Theta / (1 + \beta \Theta)]}{1 + \kappa_B Y_B \exp[\alpha_k \beta \Theta / (1 + \beta \Theta)]} \quad (33)$$

EXPERIMENTAL

The experimental system has been described in^{1,2}. As a model system the hydrogenation of benzene on a Ni catalyst (Ni/alumina, 58% Ni) and thiophene as a poison has been chosen. The experiment presented in this paper corresponds to the operating conditions given in Table I.

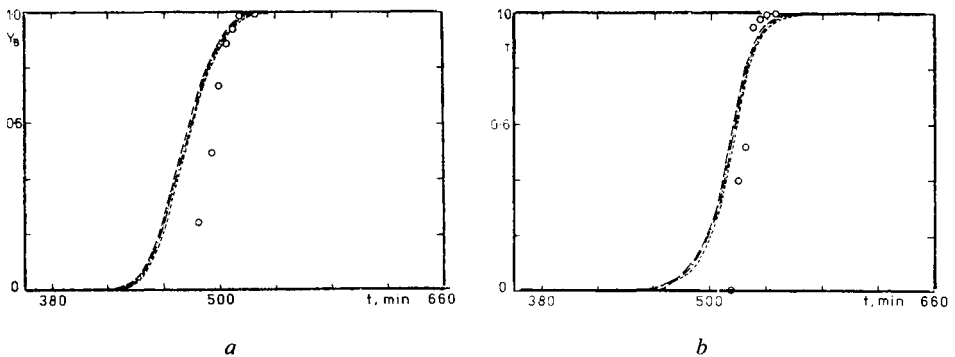


FIG. 6

Comparison of experiment and Model 3 for various values of k_{gJ} . Run 3. ($k_D = 0.09754 \text{ m}^3 \cdot \text{s}^{-1}$). \circ Experiment, $\cdots \cdots$ $k_{gJ} = 0.016 \text{ m s}^{-1}$, $-----$ $k_{gJ} = 0.014 \text{ m s}^{-1}$, $-----$ $k_{gJ} = 0.01509 \text{ m s}^{-1}$

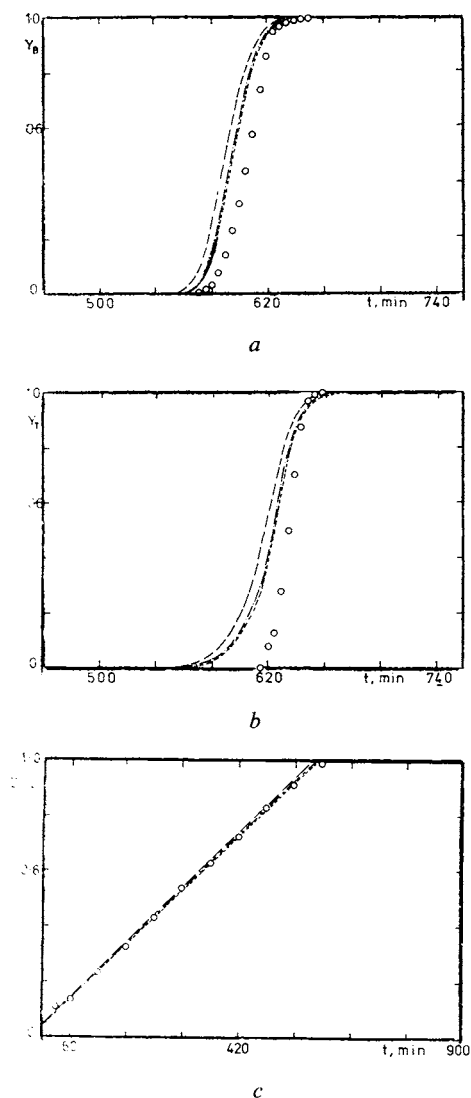


FIG. 7

Comparison of experiment and Model 3 for various values of k_{gJ} . Run 5. ($k_{D1} = 0.1276 \text{ m}^3 \text{ mol}^{-1} \text{ s}^{-1}$) \circ Experiment, $\cdots\cdots\cdots$ $k_{gJ} = 0.02216 \text{ m s}^{-1}$ and $k_{gJ} = 0.024082 \text{ m s}^{-1}$, $-----$ $k_{gJ} = 0.020 \text{ m s}^{-1}$, $-\cdot-\cdot-\cdot-$ $k_{gJ} = 0.016 \text{ m s}^{-1}$. a) Exit benzene concentration vs time. b) Exit thiophene concentration vs time. c) Point of temperature peak vs time

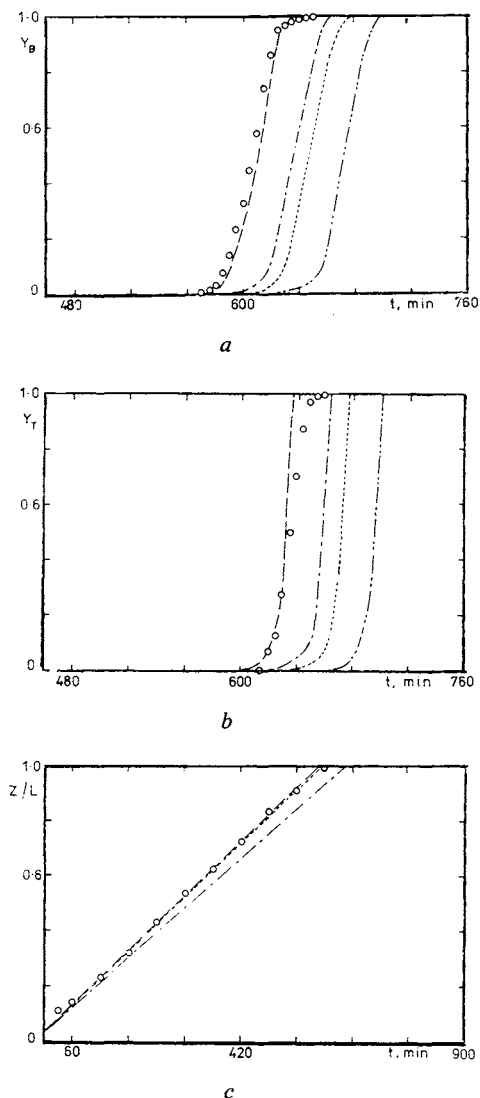


FIG. 8

Comparison of experimental and Model 1 for various values of k_{gJ} . Run 5. \circ Experiment, $-----$ $k_{gJ} = 0.016 \text{ m s}^{-1}$, $-\cdot-\cdot-\cdot-$ $k_{gJ} = 0.020 \text{ m s}^{-1}$, $\cdots\cdots\cdots$ $k_{gJ} = 0.02216 \text{ m s}^{-1}$, $-\cdot-\cdot-\cdot-$ $k_{gJ} = 0.02408 \text{ m s}^{-1}$. a) Exit benzene concentration vs time. b) Exit thiophene concentration vs time. c) Point of temperature peak vs time

The numerical values of the kinetic rate equation parameters (k_∞ , K_∞ , E , Q , k_g , k_D , D_j) have been obtained from rotating basket reactor measurements⁷ (Table II). The mass and heat transfer coefficients (k_{gB} , k_{gJ} , h_f) have been estimated from the Hougen correlations for j_M and j_H factors suggested by Saterfield⁸. The overall heat transfer coefficient has been evaluated from the coincidence of model and experimental results. The number of regions has been estimated by the rule, that the length of one region has to be equal to the pellet diameter. The numerical values of these parameters are listed in Table III.

Numerical Solution

The well-mixed regions in series model with shell progressive decay mechanism has been solved by the following iterative procedure: Compute $Y_{ji}^*(\tau)$ from Eqs (11), (15), (16) (where $\varphi = \varphi(\tau)$) and $\varphi(\tau + \Delta\tau)$ from Eq. (11) by the explicit finite difference scheme. Compute $Y_{ji}^*(\tau + \Delta\tau)$

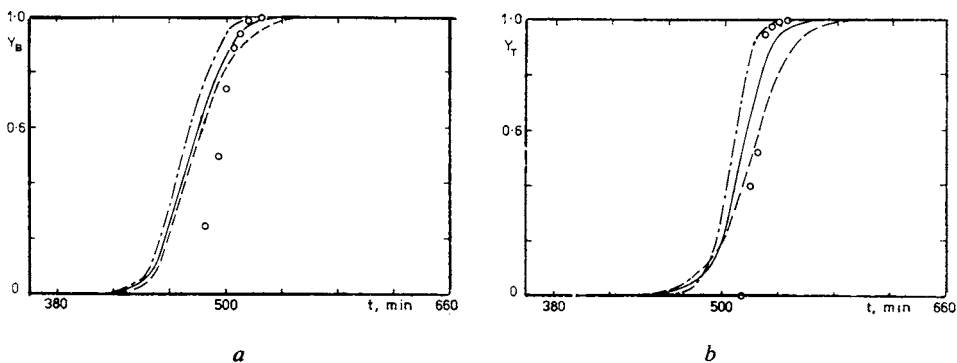


FIG. 9

Comparison of experiment and Model 3 for various values of k_{D1} ($k_{gJ} = 0.1509 \text{ m s}^{-1}$). Run 3. \circ Experiment, — $k_{D1} = 0.09754 \text{ m}^3 \text{ mol}^{-1} \text{ s}^{-1}$, - - - $k_{D1} = 0.130 \text{ m}^3 \text{ mol}^{-1} \text{ s}^{-1}$, $\cdots\cdots\cdots$ $k_{D1} = 0.060 \text{ m}^3 \text{ mol}^{-1} \text{ s}^{-1}$. a) Exit benzene concentration vs time. b) Exit thiophene concentration vs time

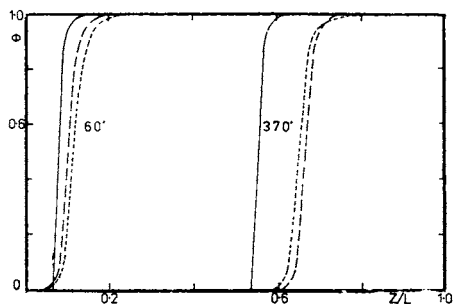


FIG. 10

The activity profiles in the reactor. Run 4. — Model 1, - - - Model 2, $\cdots\cdots\cdots$ Model 3. Curves parametrized by t , min.

from Eqs (11), (15), (16) (now $\varphi = \varphi(\tau + \Delta\tau)$) and new approximation of $\varphi(\tau + \Delta\tau)$ from Eq. (11) by the implicate finite difference scheme. Repeat the last step until satisfactory coincidence is achieved. In such a way compute the active core radius and poison concentration profiles along the reactor (for $i = 1, \dots, N$). To obtain the key component concentration and temperature profiles at time $\tau + \Delta\tau$, solve the nonlinear Eqs (12), (13), (18) and (18) for $i = 1, \dots, N$ using Newton's method.

TABLE V
Influence of k_{gJ} on models 1 and 3

Run 5		Model 1, Fig. 8			Model 3, Fig. 7		
k_{gJ} m s^{-1}	t_1^0 min	ω_{11}	ω_{12}	ω_{13}	t_2^0 min	ω_{31}	ω_{32}
0.022	8.352	0.182	0.805	0.012	7.082	0.683	0.317
0.024	7.816	0.195	0.792	0.013	6.903	0.701	0.299
0.020	9.079	0.168	0.821	0.011	7.323	0.661	0.339
0.016	10.943	0.140	0.851	0.009	7.945	0.609	0.391

TABLE VI
Influence of k_{gJ} and k_{D1} on model 3

Run 3		$k_{D1} = 0.09754 \text{ m}^3 \text{ mol}^{-1} \text{ s}^{-1}$		
k_{gJ} m s^{-1}	t_2^0 min	ω_{31}	ω_{32}	
0.0151	6.926	0.663	0.337	
0.0140	7.108	0.646	0.354	
0.0160	6.794	0.676	0.324	
Run 3		$k_{gJ} = 0.0151 \text{ m s}^{-1}$		
k_{D1} $\text{m}^3 \text{ mol}^{-1} \text{ s}^{-1}$	t_2^0 min	ω_{31}	ω_{32}	
0.130	5.780	0.596	0.404	
0.098	6.926	0.663	0.337	
0.060	9.799	0.762	0.238	

A similar iterative procedure for solution of the well-mixed regions in series model with uniform decay mechanism has been employed.

RESULTS AND DISCUSSION

Figs 1–5 illustrate fits of particular models with all the experimental runs (the displayed variables being exit benzene and thiophene concentrations, point of temperature peak *vs* time and transient temperature profiles). As a criterion of adequacy we choose the difference between computed and experimental time in which exit benzene concentration is equal to 0.5. The values of the criterion δ for all runs and models are in Table IV. The best agreement of exit benzene and thiophene concentrations between model and experimental has been obtained for the two site model for thiophene chemisorption, the difference between uniform mechanism of deactivation with one and two types of active sites not being significant. The criterion δ has the highest value for the shell progressive model. It is due to the model sensitivity to the estimated value of k_{gJ} (Table V, Figs 7 and 8). This sensitivity is due to the fact, that the reactor was packed by small catalyst pellets for which the rate controlling step is external diffusion while internal diffusion is negligible. On the other hand, the rate controlling step for the two site model is chemisorption of the poison, hence the model is less sensitive on the estimation of the values k_{gJ} (Table V and VI, Figs 6, 7 and 9).

In Fig. 10 the activity profiles in the reactor for the described models are displayed. For the shell progressive model 1 one can see only a narrow region in which activity changes from zero to one. This leads to a higher value of temperature maximum.

From the figures mentioned above one concludes that the heterogeneous models of well-mixed regions in series provide for a good description of the catalytic fixed bed reactor and deactivation process. Satisfactory agreement of outlet concentrations and hot spot movement and good qualitative description of the temperature profile has been achieved.

LIST OF SYMBOLS

A_w	heat exchange surface (m^2)
a_J	poison adsorbed amount ($mol\ kg^{-1}$)
a_J^*	equilibrium poison adsorbed amount ($mol\ kg^{-1}$)
a_v	external pellet surface (m^2)
c	concentration ($mol\ m^{-3}$)
c_p	heat capacity ($J\ kg^{-1}\ K^{-1}$)
D	diffusion coefficient of catalyst ($m^2\ s^{-1}$)
E	activation energy of catalytic reaction ($J\ mol^{-1}$)
$F_w = h_w A_w / (\dot{V} \rho_g c_{pg})$	dimensionless overall heat transfer coefficient
$F_t = h_t a_a / (\dot{V} \rho_g c_{pg})$	dimensionless parameter, see Eq. (17)
$F_s = \frac{\xi_w^0}{\xi_w} \rho_g c_{pg} \rho_s R / (3h_t c_{BO})$	dimensionless parameter, see Eq. (18)

- $G_g = k_{gJ} a_v / \dot{V}$ dimensionless parameter, see Eq. (15), (23)
 $G_{s1} = a_J^* \rho_s R / (k_{gJ} c_{J0} t_1^0)$ dimensionless parameter, see Eq. (16)
 $G_{s2} = a_J^* \rho_s R / (k_{gJ} c_{J0} t_2^0)$ dimensionless parameter, see Eq. (24)
 $(-\Delta H)$ heat of reaction (J mol^{-1})
 h_f heat transfer coefficient ($\text{J m}^{-2} \text{s}^{-1} \text{K}^{-1}$)
 L length of the reactor (m)
 k_∞ frequency factor of catalytic reaction ($\text{mol kg}^{-1} \text{s}^{-1} \text{Pa}^{-1}$)
 k_D deactivation rate constant ($\text{m}^3 \text{mol}^{-1} \text{s}^{-1}$)
 k_{D1} deactivation rate constant ($\text{m}^3 \text{mol}^{-1} \text{s}^{-1}$)
 k_s surface reaction rate constant (m s^{-1})
 k_g gas phase mass transfer coefficient (m s^{-1})
 N number of well-mixed regions
 P partial pressure (Pa)
 Q adsorption heat of benzene (J mol^{-1})
 R radius of catalyst pellet (m)
 r^j active core radius (m)
 T temperature (K)
 T_c ambient temperature (K)
 t time (s)
 $t_1^0 = \rho_s a_J^* R (1/k_s + 1/k_{gJ} + R/D_J) / c_{J0}$ characteristic deactivation time (s)
 $t_2^0 = 1/(k_D c_{J0}) + R \rho_s a_J^* / (3k_{gJ} c_{J0})$ characteristic deactivation time (s)
 \dot{V} volumetric flow rate ($\text{m}^3 \text{s}^{-1}$)
 Y dimensionless concentration, $Y = c/c_0$
 $Z_g = k_{gB} a_v / \dot{V}$ dimensionless parameter, see Eq. (13)
 $Z_s = -v_B R \rho_s \xi_W^0 / (3k_{gB} c_{B0})$ dimensionless parameter, see Eq. (14)
 $\alpha_i = E_i / (RT)$ dimensionless parameter, Eq. (27)
 $\alpha_k = Q / (RT)$ dimensionless parameter, Eq. (17)
 $\beta = (-\Delta H) c_{B0} / (q_g c_{pg} T_0)$ dimensionless parameter, Eq. (27)
 ν stoichiometric coefficient
 $\dot{\xi} = \xi_W / \xi_W^0$ dimensionless reaction rate
 $\dot{\xi}_W$ rate of catalytic reaction ($\text{mol s}^{-1} \text{kg}^{-1}$)
 ξ_W^0 reaction rate on the fresh catalyst (inlet conditions) ($\text{mol s}^{-1} \text{kg}^{-1}$)
 $\kappa_B = K_\infty P_{B0} \exp(-\alpha_k)$ dimensionless parameter, Eq. (27)
 ρ density (kg m^{-3})
 Φ catalyst activity
 $\phi = r^j / R$ dimensionless active core radius
 $\Theta = (T - T_0) \rho_g c_{pg} / ((-\Delta H) c_{B0})$ dimensionless temperature
 $\omega_{11} = \rho_s a_J^* R / (c_{J0} k_s t_1^0)$ dimensionless parameter, see Eq. (11)
 $\omega_{12} = \rho_s a_J^* R / (c_{J0} k_{gJ} t_1^0)$ dimensionless parameter, see Eq. (11)
 $\omega_{13} = \rho_s a_J^* R^2 / (c_{J0} D_J t_1^0)$ dimensionless parameter, see Eq. (11)
 $\omega_{21} = 1 / (k_D c_{J0} t_2^0)$ dimensionless parameter, see Eq. (22)
 $\omega_{22} = \rho_s a_J^* R / (3k_{gJ} c_{J0} t_2^0)$ dimensionless parameter, see Eq. (22)
 $\omega_{31} = 1 / (k_{D1} c_{J0} t_2^0)$ dimensionless parameter, see Eq. (28)
 ω_{32} dimensionless parameter, see Eq. (28), $\omega_{32} = \omega_{22}$

Subscripts

- B benzene
 g gas phase
 J poison

- H hydrogen
s catalyst pellet
0 inlet
1 shell progressive mechanism
2 uniform mechanism

Superscripts

- * gas phase
j active core
p pellet surface

REFERENCES

1. Ilavský J., Brunovská A., Valtýni J., Buriánek J.: Chem. Papers 4, 433 (1983).
2. Markoš J., Brunovská A., Ilavský J.: Chem. Papers, in press.
3. Barto M., Brunovská A., Ilavský J.: Chem. Papers, in press.
4. Khang S. J., Levenspiel O.: Ind. Eng. Chem. Fundam. 12, 185 (1977).
5. Wheeler A., Robell A. J.: J. Catal 13, 299 (1969).
6. Froment G. F., Bischoff K. B.: *Chemical Reactor Analysis and Design*. Wiley, New York 1979.
7. Markoš J., Brunovská A., Ilavský J.: Chem. Papers, in press.
8. Satterfield C. N., Sherwood T. K.: *The Role of Diffusion in Catalysis*. Adison-Wesley, Reading, Ma., 1963.